Journal of Microscopy

Journal of Microscopy, Vol. 241, Pt 3 2011, pp. 303–314
Received 14 August 2009; accepted 7 July 2010

doi: 10.1111/j.1365-2818.2010.03441.x

Cell counting tool parameters optimization approach for electroporation efficiency determination of attached cells in phase contrast images

M. USAJ*, D. TORKAR†, M. KANDUSER* & D. MIKLAVCIC*
**Faculty of Electrical Engineering, University of Ljubljana, Ljubljana, Slovenia*
†Jozef Stefan Institute, Ljubljana, Slovenia

Key words. Artificial neural networks, backpropagation, biomedical image processing, electroporation, microscopy, object detection, optimization, V79 cell line.

Summary

In this paper a novel parameter optimization approach for cell detection tool and counting cells procedure in phase contrast images are presented. Manual counting of the attached cells in phase contrast images is time-consuming and subjective. For evaluation of electroporation efficiency of attached cells, we often perform manual counting of the cells which is needed to determine the percentage of electroporated cells under different experimental conditions. Here we present an automated cell counting procedure based on novel artificial neural network optimization of Image-based Tool for Counting Nuclei algorithm parameters to fit the training image set based on counts from an expert. Comparing the results of automated cell counting to user manual counting a 90,31% average agreement was achieved which is reasonably good especially taking into account inter-person error which can be up to 10%. Even more, our procedure can also be used for fluorescent cell images with similar counting accuracy (>90%) enabling us to determine electroporation efficiency. In our experiments, the electroporation efficiency determined by manual cell counting was virtually the same as the one obtained by the automated procedure.

Introduction

Electroporation (Weaver & Chizmadzhev, 1996), also termed electropermeabilization (Rols & Teissie, 1992), is an efficient method for transient increase of cell membrane permeability, which is widely used for drug and gene delivery into the living cells. The method is highly efficient and does not include the exposure of cells to chemical, viral or any kind of toxic additives (Rols, 2006). Membrane permeabilization is obtained by application of strong external electric field to cells or tissues (Tsong, 1991; Teissie & Rols, 1993). With careful selection of electric pulse parameters such as pulse amplitude, duration and number, we can obtain transient permeabilization, which does not affect cells viability (Neumann *et al.*, 1989; Canatella *et al.*, 2001). Electroporation is used in many biomedical applications; the most interesting at present are electrochemotherapy of tumours (Gehl & Geertsen, 2006; Marty *et al.*, 2006; Mir *et al.*, 2006; Sersa *et al.*, 2008), gene electrotransfer (Neumann *et al.*, 1999; Andre & Mir, 2004; Golzio *et al.*, 2004; Pavselj & Preat, 2005), cell fusion (Hayashi *et al.*, 2002; Trontelj *et al.*, 2008; Yu *et al.*, 2008; Gabrijel *et al.*, 2009) and nonthermal irreversible electroporation (Rubinsky *et al.*, 2007; Zupanic & Miklavcic, 2010).

For the study of basic mechanisms of electroporation and its biomedical applications, researchers often perform experiments on cell cultures *in vitro*. Even though cell membrane permeabilization can be determined by different already established methods such as flow cytometry or spectrofluorimetry, those methods are only applicable when cells in suspension are used. In such experiments, all cells in the population have roughly the same shape and are therefore affected in the same manner by the electric field. Nevertheless, in many cases experiments performed on adherent cells are needed. Adherent cells maintain their shape and intact internal structure (cytoskeleton) and the results obtained in those cells are comparable better to real *in vivo* situation (at least for a simple homogeneous tissue) than results from cell suspensions (Kandušer & Miklavčič, 2009). Another advantage of the experiments performed on attached cells is the fact that they can be observed under inverted microscope for longer time and cell responses to electric pulses can be detected *in situ*. For any further studies of electroporation-based treatments, the first condition is determination of the

Correspondence to: D. Miklavcic, Faculty of Electrical Engineering, University of Ljubljana, Trzaska 25, SI-1000, Ljubljana, Slovenia. Tel: +386-1-4768-456; fax: +386-1-4264-658; e-mail: damijan.miklavcic@fe.uni-lj.si

© 2010 The Authors
Journal of Microscopy © 2010 The Royal Microscopical Society

percentage of permeabilized cells with different fluorescent dyes such as propidium iodide or lucifer yellow (Macek-Lebar & Miklavcic, 2001; Pucihar *et al.*, 2002). This percentage is often determined by manual counting of cells on phase contrast images and corresponding number of permeabilized cells is detected by fluorescence microscopy. Thus, both images, phase contrast and fluorescence ones, have to be counted separately, which means that we cannot used established fluorescent immunehistochemical staining methods (Chen *et al.*, 2006; Steenstrup *et al.*, 2000;). Manual counting of cells is time-consuming and subjective. Namely, intra-person variation and inter-person variation of counted number of objects in such images are not negligible (Jacobs *et al.*, 2001; Embleton *et al.*, 2003).

Cell detection in phase contrast images for experimental results evaluation is a key problem. A typical phase contrast images of adherent cells have the following characteristics: (1) noise and artefacts, (2) various cell shapes and cell intensity overlapping due to complexity of cellular topologies, (3) internal cell structures with a lower intensity, (4) cells in close contacts, therefore cell boundaries are not seen clearly and (5) varying density of cell culture resulting from nonuniform distribution of cells in the culture (Yongming *et al.*, 1999; Li *et al.*, 2006). All these characteristics lead to a decreased contrast between cells and background. In addition, equipment-related factors, which contribute to the quality of the image, such as uneven illumination and electronic or optical noise, also play an important role in the effective segmentation of a digital image (Haralick & Shapiro, 1985). All problems mentioned earlier are also found in live cell imaging and can contribute to poor image quality for automated image processing, leading to image analysis problems that remain inadequately solved. The segmentation approach adopted must be robust against possible problems related to phase contrast image to ensure that reliable information about cell number is obtained (Haralick & Shapiro, 1985).

Several digital image segmentation techniques were investigated for cell detection in phase contrast images, such as contour-based, region-based and mixed contour-based methods, histogram-based with minimum-error-threshold and watershed algorithm. For phase contrast images, however, none of the above-mentioned methods can be used directly. Effective detection by means of digital image segmentation techniques requires certain object characteristics such as clear object borders, distinguished textures, colours or topologies that have to be present in all images used for automated cell counting (Haralick & Shapiro, 1985; Wu *et al.*, 1995; Yongming *et al.*, 1999; Debeir *et al.*, 2005; Ambriz-Colin *et al.*, 2006; Yang *et al.*, 2006). Sometimes specific algorithms or method modifications are needed for counting a particular cell lines, for example white blood cells (Theera-Umpon & Gader, 2002; Wang & Min, 2006).

There are some commercial software products available and they provide object-counting and feature detection [MetaMorph (Molecular Devices, Downingtown, PA, U.S.A.), Bioquant (Image Analysis Corporation, Nashville, TN, U.S.A.), Image-Pro (Media Cybernetics, Bethesda, MD, U.S.A.) and also freeware ImageJ (U.S. National Institutes of Health, Bethesda, MD, U.S.A.), UTHSCSA ImageTool (University of Texas Health Science Center, San Antorio, TX, U.S.A.)]. All these tools, however, often fail to provide reliable results in term of accurate cell detection and/or require intensive user interaction to obtain initialization or parameter settings for accurate results (Byun *et al.*, 2006). Usual approach within these programs is to apply several global image-processing techniques (various image filtering and edge detection algorithms) to create binary images where object counting is finally performed. For phase contrast image with very dissimilar objects (e.g. attached cells) global image processing techniques are not sufficient. In our opinion, local image-processing methods (e.g. template matching) could be more suitable in such cases.

Image-processing techniques usually have a large amount of parameters, which have to be precisely tuned to get reliable results. In phase contrast images, characteristic of individual adherent cells differ significantly one from another. Therefore, results can be heavily skewed by software tuning. Cells on phase contrast images due to all mentioned issues earlier usually do not have any characteristic dominating adherent shape and other optical properties, thus it is difficult to obtain good parameter set.

However, some optimization strategies exist, which can be used to search for optimal parameters of given algorithm. The artificial neural network (ANN) represents a general computing mechanism able to perform different tasks such as classification, function approximation, prediction and optimization. A widely used topology (ANN structure) in different domains is a multilayer perceptron. It consists of neurons organized in layers. The inputs are grouped in an input layer, outputs in an output layer and all the other units in so called hidden layers that 'cannot be seen' neither from the input nor from the output of the network. All links are made among units in different layers from the input side towards the output side of the network. Connections within the same layer or backward connection from a layer closer to output to layers further from the output are forbidden. All links within the network are weighted with weights usually residing between 0 and 1.

ANN can be trained using the backpropagation training method that uses backpropagation of a network error to compute the gradient of an error function with respect to the network weights. The algorithm repeatedly adjusts the weights to minimize the mean square error between the actual output vector and the desired network output vector. When the desired output vector is known, this method belongs to a family of supervised learning rules (with a 'teacher').

© 2010 The Authors

The traditional backpropagation implies a deterministic optimization algorithm called *direct gradient descent*, but can be replaced with other, more advanced methods (Masters, 1995). The weights are changed by an amount proportional to error gradient. The proportional factor is denoted as a *learning rate* and the weight changes are corrected by a *momentum* (decay) factor to control the velocity of the point in the weight space. Using this, the local minima in the error minimization procedure are more successfully avoided (Rumelhart *et al.*, 1986). Although there exists a relationship between the gain of the activation function, learning rate and initial weights (Thimm *et al.*, 1996), these factors and the net topology are usually chosen either experimentally or using some existing thumb rules. Recently, the genetic algorithm received much attention in determination of the optimal network parameters.

The aim of this study was to develop technique for effective automated counting of attached cells in phase contrast images that could be used later on for live cell imaging. In such cases, the analysis of large number of images obtained by automatic image acquisition which are not all of the same quality is required. We first identified the algorithm in ITCN (Image-based Tool for Counting Nuclei, Centre for Bio-Image Informatics, University of California) for appropriate cells detection tool in phase contrast images (Usaj *et al.*, 2007). The ITCN algorithm requires set up of three (optimal) parameters to effectively perform cell counting. Optimal algorithm's parameters are set up with minor initial expert input followed by the optimization approach, which includes ANN. We introduced a novel solution, where network input is fed by normalized procedure error and network outputs are algorithm (ITCN) parameters. With this approach we shortened counting time (from 8 to 9 h to 18 min) and obtained 90.31% accuracy from our phase contrast image database. Finally, we tested this procedure on real electroporation experimental data and obtained good results.

Material and methods

Electroporation experiments

A cell line V-79 Chinese hamster lung fibroblasts (ECACC, Salisbury, U.K., EU) was used in experiments. Cells were grown in an Eagle's minimum essential medium supplemented with 10% foetal bovine serum (Sigma, St. Louis, MO, U.S.A.) at 37°C in a humidified 5% CO_2 atmosphere in an incubator (Kambic, Semic, Slovenia) For experiments cells were plated previous day in 24 multiwell microplate (TPP, Trasadingen, Switzerland) in concentration 4×10^4 cells per well. Immediately before electric pulse application, the growth medium was replaced with phosphate buffer containing 0.15 mM propidium iodide. Electric pulses were applied with electric pulse generator Cliniporator (Igea, Carpi, Italy) using wire electrodes 5 mm apart (Fig. 1).

Electric pulse parameters were: 8 pulses, duration 100 μs and repetition frequency 1 Hz. The pulse amplitude was increased from 0 V cm^{-1} for control treatment, and from 200 to 800 V cm^{-1} in 100 V cm^{-1} steps. The phase contrast and fluorescent images of the treated cells were captured using cooled CCD camera (Visicam 1280, Visitron, Puchheim, Germany) mounted on a fluorescence microscope (Zeiss AxioVert 200, objective 20×, Zeiss, Oberkochen, Germany) using MetaMorph 5.0 software (Molecular Devices Corporation, PA, U.S.A.), exposure time 100 ms. For each parameter, five phase contrast and corresponding fluorescent images were acquired from three independent experiments giving final number of 120 phase contrast images. For our procedure evaluation, we use additional phase contrast images acquired from other four similar experiments at the same conditions from which we formed original database of 304 images. Then we discarded those with poor focus (96). We can avoid poor focus with proper microscopy set up and for that reason we excluded those images from automated counting procedure. We performed this task manually because automated exclusion of images with poor focus is not the aim of our paper. From all remaining phase contrast images (208), we created test image database as described in the next section. Evaluated algorithm was then applied to our electroporation experiments on attached V-79 cells. The acquired images had the resolution of 640 × 512 pixels and 256 greyscale (8-BPP).

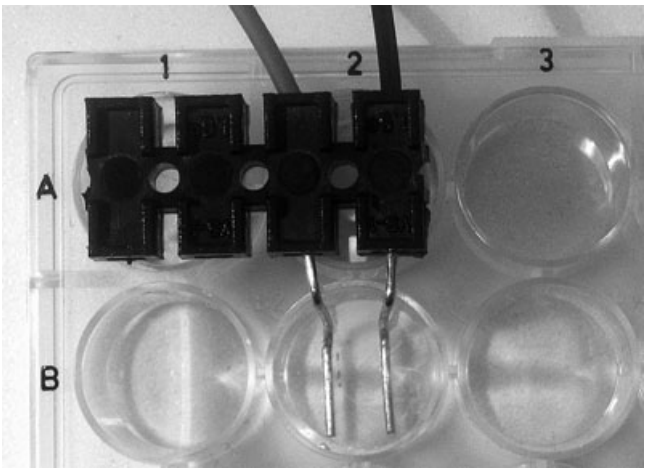

Fig. 1. Experimental set up of platinum electrodes in 24-well microplate for electroporation of attached cells. The distance between platinum (Pt/Ir = 90/10) wire electrodes is 5 mm.

Creating phase contrast image database

From our initial database (208 images from seven independent experiments), we discarded those with huge artefacts such as rubbish or dirties (3), those with giant and/or fused cells (35) and those with clustered remainders of cells (12). The remaining 158 (76%) phase contrast images – our test data (examples of those images we can see in Fig. 2) – included images with similar cell area, but still with very different cell shapes and density. Image files were then named

© 2010 The Authors

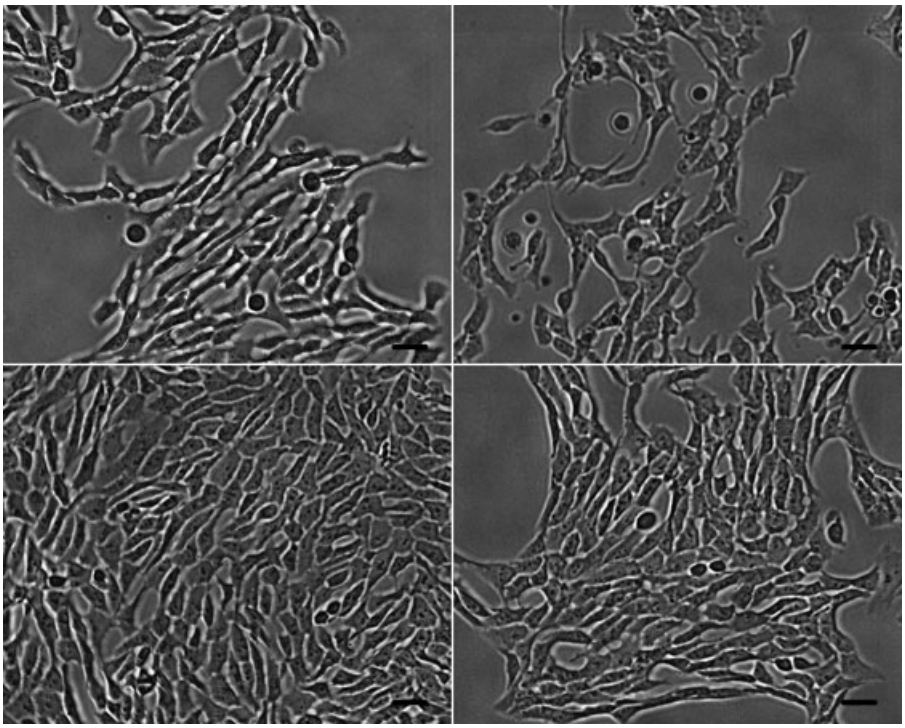

Fig. 2. Examples of phase contrast images of attached cells with different cell density (126 cells/image – top right to 329 cells/image – bottom left) from our image database. Images were captured under 20× objective magnification. Scale bar corresponds to 40 μm.

and preprocessed. Automatically counted cell numbers were compared to manual counting obtained by average results of three experts – our ground truth. We have determined inter-person error as average of relative standard deviations. Second inter-person error is determined also as average of relative standard deviation on ten manually counted images by eight people from our laboratory who work regularly with cells as researchers and are therefore used to count cells under phase contrast microscopy (in range: Ph.D. students, post docs, teaching assistants).

Image preprocessing

In our counting procedure, we integrated two preprocessing steps: shading correction (to improve image quality) and histogram equalization (to enhance contrast between cells and background).

Shading correction. Microscopic images exhibit significant intensity nonuniformity, often referred to as shading or intensity inhomogeneity (Russ, 1995; Tomazevic *et al.*, 2002; Vovk *et al.*, 2007). Among many shading correction methods, we have chosen retrospective shading correction based on entropy minimization to improve image quality (Likar *et al.*, 2000). By contrast to other retrospective methods, the selected method deals successfully with both multiplicative and additive shading components and in a great variety of differently structured images. Briefly, linear image formation model was created, which consists of an additive and multiplicative parametric component. Shading correction was then performed by the inverse of the image formation model, which shading components were estimated retrospectively by minimizing the entropy of the acquired images.

Histogram equalization. On images with corrected intensity inhomogeneity histogram equalization was applied to enhance contrast between cells and background. This preprocessing step was integrated in our counting procedure as a consequence of thorough comparison of counting results using histogram equalization to the ones not using it. For contrast enhancement we use MATLAB (MathWorks, Natick, MA, U.S.A.) function for contrast-limited adaptive histogram equalization (CLAHE), which enhances the contrast of the greyscale image. CLAHE operates on small regions in the image, called tiles, rather than the entire image. We specified 15 tiles per each row and each column. Total number of tiles was thus 225. Each tile's contrast was enhanced, so that the histogram of the output region approximately matches the histogram specified by the 'Distribution' parameter, in our case Bell-shaped histogram.

Automated cell detection

For automated cell detection, we used algorithm implemented within the ITCN tool. The algorithm is described in details elsewhere (Byun *et al.*, 2006). Briefly, the algorithm requires

© 2010 The Authors

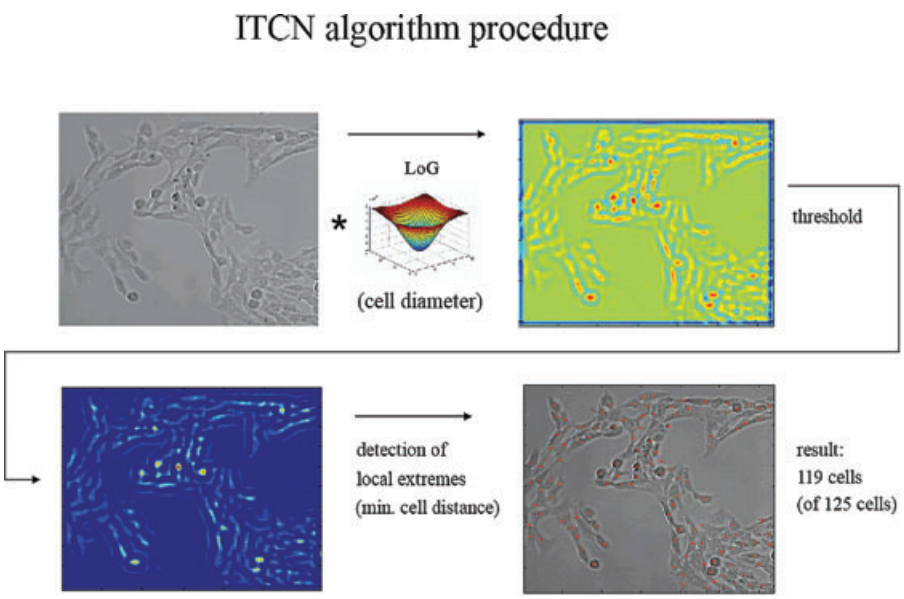

Fig. 3. Cells detection procedure realized in Image-based tool for counting nuclei (ITCN) algorithm: an input image is convoluted with Laplacian of Gaussian (LoG) then the convoluted image is thresholded, and finally a detection of local extremes is performed.

three parameters: (1) cell diameter, (2) minimal cell distance and (3) filter threshold. Objects (cell nuclei originally, cells in our study) in the image are detected using a template matching approach where the object model is convoluted with an image and in each position the correlation factor is calculated. Within ITCN Laplacian of Gaussian (LoG) is used as cell detector with the diameter proportional to mean cell size. The result of the convolution is a smooth continuous image where object centres are represented by local extremes. Afterwards, a threshold is applied to image to remove false local extremes occurring, for example from empty space surrounded by cells. Remaining extremes are detected using minimal cell-to-cell distance. The procedure is depicted in Fig. 3.

The ANN initialization

Among various ANN structures, we selected a multilayer perceptron. The topology of the created ANN consists of one processing unit (neuron) in the input layer and is fed by the normalized relative automated counting error. The output layer contains three neurons, one for each ITCN parameter. The number of neurons in the hidden layer was defined experimentally and set to 10. ANN was trained using the backpropagation training method. A 'quickprop' gradient search algorithm for ANN training was used mainly due to its advantages in speed. The proportional factor (learning rate) was set to 0.1 and the momentum (decay) was set to 0.5.

Smart parameter optimization procedure

We tested several optimization approaches to obtain optimal parameter. The parameters search space was reasonably constrained with respect to cells/images characteristic (cell diameter and minimal distance/threshold). The search space was equally discretized (Table 1), which gave a total of 2541 sets of parameters. We tested different sampling procedures; in the first step we took every value of parameters. In the next step, we took only every second (third, fourth, fifth) value of parameters (each time the border parameters values however were included), which gave reduced sets of parameters' values. Finally, we took only border values of parameter and the middle one (three values of each parameter) which gave 27 combinations (sets) of parameters' values.

Table 1. Parameter search space boundaries.

Cell diameter (pixels)	[25–35]; step 1
Minimal distance (pixels)	[15–25]; step 1
Threshold	[0.05–0.25]; step 0.01

The whole optimization procedure consisted of the following steps. At the beginning, the training set was generated using only three images with known cell numbers randomly selected out of 158 images (less than 2% of all images). The three parameters, required by ITCN algorithm, were varied within preselected boundaries and inner points determined by sampling procedure. For each instance, the image processing of the selected (training) images were performed and the number of cells determined. All combinations of sets of parameters and numbers of counted cells (true and automated) were randomized and then used to compose a different data for ANN training and validation. A training data consisted of 60% of samples, a cross validation data of 15% and a test data of 25%.

© 2010 The Authors

Our novel idea was to train the network with the training data values and then set the input (normalized relative automated counting error) to zero and the outputs should give optimal values of the three ITCN algorithm's parameters. If the ANN was chosen well (having good generalization ability) these values should be optimal for the whole test images.

The procedure was tested on 10 different training sets of images (on PC Pentium(R) D CPU 3 GHz, 1 GB of RAM, Windows XP) and mean relative error as well as mean standard deviation were determined. For each set, the ANN was trained for 10 000 cycles (epochs) where in each epoch all the samples from the training set was exposed to the network inputs.

Procedure's performance and accuracy

Exhaustive global optimization. To evaluate our optimization approach described in previous subsection, we performed a global parameters optimization that yielded global optimal parameter set (in our defined parameter space). In this case, training set was equal to data set that means all 158 images were included in optimization. The three parameters required by ITCN algorithm were varied within preselected boundaries with all samples included. For each instance, the image processing of all images was performed and the number of cells determined. The parameter set, which minimized absolute relative error, was chosen as global optimal parameter set and its error as global minimal error. The same computer as in previous section was used. The time needed for completing global optimization was 3 weeks.

Absolute relative error. The results of counting cell procedure were presented by the error computed according to the Eq. (1)

$$E = \frac{1}{N}\sum_{N}\frac{|\mathrm{ND} - \mathrm{GT}|}{\mathrm{GT}}, \qquad (1)$$

where E is an average absolute relative number-of-cells error, N is the number of images in the set, ND and GT is the number of cells detected by our automated procedure and by manual counting, respectively.

Evaluation of procedure on our data obtained from electroporation experiments

We finally applied our counting procedure to three electroporation experiments. From each experiment we got 40 phase contrast and same number of corresponding fluorescent images. The training sets consisting of three phase contrast or fluorescence images (7.5% of all images) per each individual experiment. For automated cell counting procedure, we empirically set parameter borders as shown in Table 2. With optimal parameters obtained by our optimization approach, we performed cell counting on phase contrast and fluorescent images. Automated counting of fluorescent cells was not the aim of this paper and we agree that other solutions exist for this purpose. However, we perform automated counting of fluorescent cells with our procedure just to show its flexibility and robustness to different image types. For counting cells on fluorescence images, we have to assure that ITCN is properly configured which means that we have to use inverted LoG (not original as in case of phase contrast images). Preprocessing steps for fluorescence images were similar as for phase contrast with additional background subtraction. Fluorescent images were manually counted only by one expert.

Table 2. Parameter search space boundaries for electroporation experiments.

	Phase contrast images	Fluorescent images
Cell diameter (pixels)	[25–35]; step 5	[10–30]; step 5
Minimal distance (pixels)	[15–25]; step 5	[10–20]; step 5
Threshold	[0.1–0.2]; step 0.05	[0.1–0.2]; step 0.05

Results

Smart parameter optimization

Our procedure for automated cell counting was tested on 10 different training sets, with different number of parameter sets. As presented in Table 3, the average error and average standard deviation did not significantly differ between numbers of parameter set used for ANN optimization. Because of that, the option with only 27 parameter sets was finally selected as sampling procedure for the proposed optimization approach. This procedure has demonstrated the best performance which includes counting accuracy of 90.31% and low computing time which was less than 18 min; 6 min for parameter optimization (average 5.98 min ± 0.95 min) and 4.3 s (±0.4 s) for processing each image.

Good ANN response is also shown in Fig. 4, where values of three parameters for each training set and different sampling procedure as well as values of global optimal parameters are presented. It can be seen that parameter's values are independent of sampling procedure and they are close to global optimum.

Table 3. Mean error and standard deviation for different number of parameter sets.

Number of parameter sets	Average error (%)	Average standard deviation (%)	Computing time
2541	9.17	7.18	8 h 42 min
396	9.17	7.18	1 h 42 min
200	8.97	7.30	47 min
96	8.97	7.18	30 min
45	9.93	7.44	22 min
27	9.69	7.34	<18 min

© 2010 The Authors

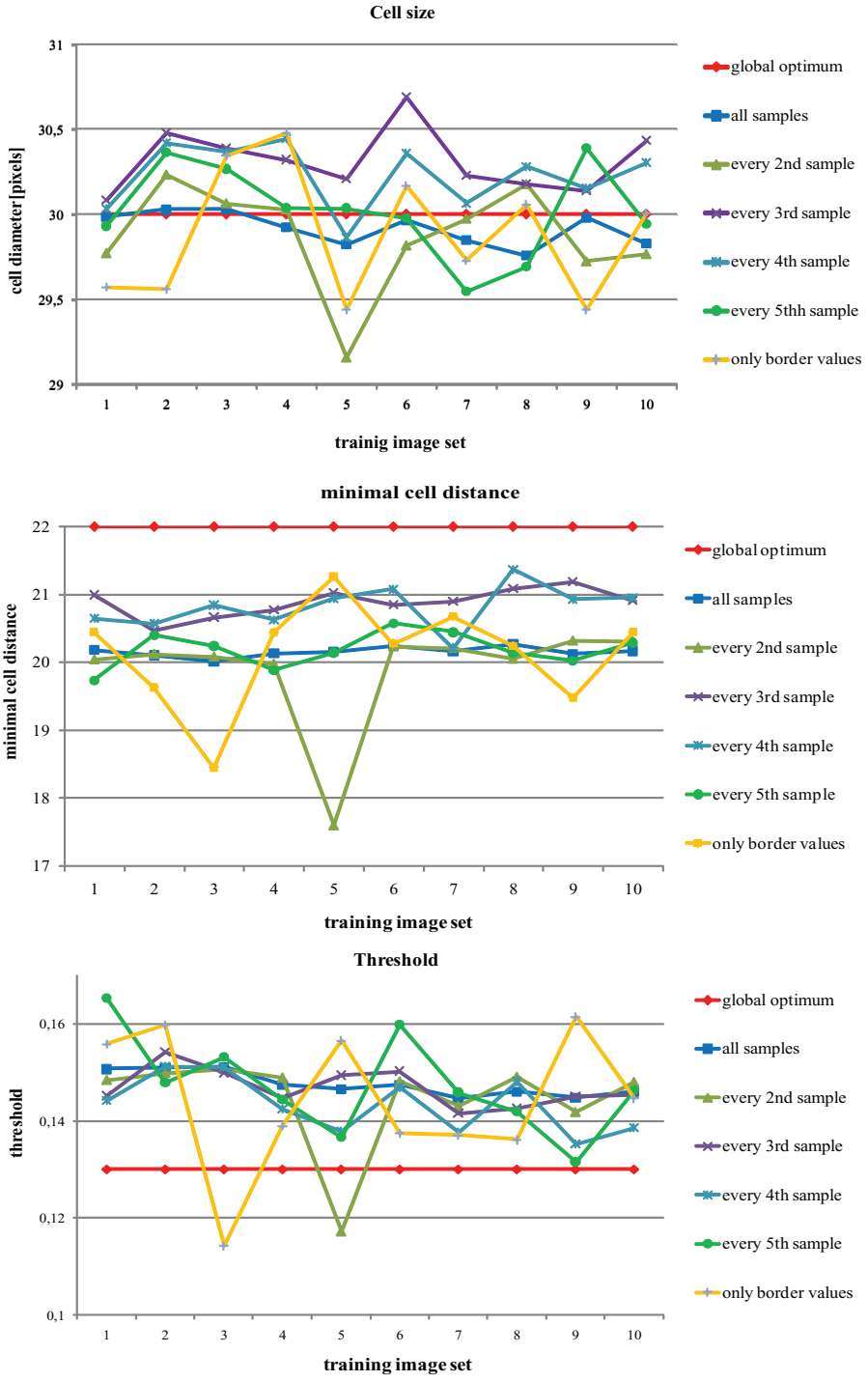

Fig. 4. The artificial neural network (ANN) optimized values for all three parameters of Image-based Tool for Counting Nuclei (ITCN) algorithm for 10 image training set and sampling procedure: cell size, minimal cell distance and algorithm's threshold.

Results of automated counting procedure for 10 different training image set show reasonably good correlation with manual counting as we see in Table 4 where absolute relative errors with SD for all 10 training image sets are presented (number of parameter sets are 27). If we performed automated counting on images without contrast enhancement using the same 10 training image set the average absolute relative error (13.02%) and SD (9.68%) are considerably higher than in the case where contrast enhancement was used (average absolute relative error 9.69% and SD 7.34%).

© 2010 The Authors

Table 4. Trend equitation, correlation coefficient and error between manual counting and automated counting (number of parameter sets are 27) for 10 training image sets.

Training set	Trend equation	Correlation coefficient R^2	Absolute relative error (%)
1	$y = 0{,}9017x$	0.8687	10.72 ± 9.03
2	$y = 0{,}9017x$	0.8687	10.72 ± 9.03
3	$y = 1{,}0262x$	0.9117	10.15 ± 7.18
4	$y = 0{,}9842x$	0.8983	9.22 ± 6.70
5	$y = 0{,}9694x$	0.8974	8.82 ± 6.59
6	$y = 0{,}9842x$	0.8983	9.22 ± 6.70
7	$y = 0{,}9546x$	0.8999	8.63 ± 6.75
8	$y = 0{,}9842x$	0.8983	9.22 ± 6.70
9	$y = 1{,}0345x$	0.8957	10.95 ± 8.01
10	$y = 0{,}9842x$	0.8983	9.22 ± 6.70
Average	$y = 0{,}9736x$	0.8935	9.69 ± 7.34

For illustration, the results of automated procedure running with optimal parameter's set obtained from one image training set (number four) are presented in Fig. 5. We can observe that there is somewhat better performance in images with fewer cells, while with increasing cells number the error becomes higher. Overall, trend equitation coefficient (0.9892) and correlation coefficient (0.8983) as well as error ($9.22 \pm 6.70\%$) still demonstrate good correlation with manual counting.

Exhaustive global optimization

We searched for global optimum parameter set to obtain global minimum error of the ITCN algorithm. Global minimum error is $7.99 \pm 6.37\%$ what is acceptable and is within the range of inter-person error. The reason for this still rather high error lies probably in large cell shape variations throughout the whole data set processed using the same parameters set of ITCN algorithm. We can also see that our procedure's average error $9.69 \pm 7.34\%$ is in the same order as global minimum error. Furthermore, it has been achieved within much shorter computer time (less than 18 min) compared to global optimum result (3 weeks).

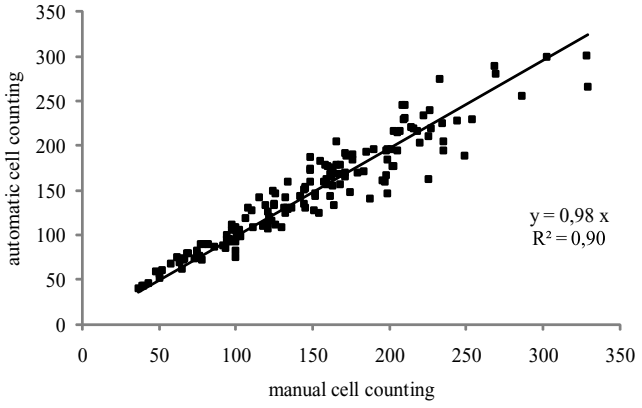

Fig. 5. Evaluation of the algorithm in all 158 images of our database. Correlation between manual and automated cell counting. Automated cell counting was performed using optimized parameters obtained from artificial neural network (ANN) optimization using data of the image training set four.

Inter-person error

For an additional evaluation of counting procedure, we determined an inter-person error among users who performed manual counting of cells. First inter-person error is an average of relative standard deviations of three manual counting of cells in all (158) images and its value (with its SD) is $6.55 \pm 3.67\%$. Second inter-person error is an average of relative standard deviations based on manual counting of cells from eight people in Laboratory of Biocybernetics on 10 images from our test images. Its value with SD is $10.57 \pm 3.25\%$, which slightly surpasses the first estimation of inter-person error. Both inter-person error are quite similar to the error of our counting procedure and clearly demonstrate difficulty to obtain real number of cells even for expert users.

In Table 5, we present the results of evaluation of our procedure: inter person errors, automatic versus manual counting, computer/human counting time.

Evaluation of procedure on our data obtained from electroporation experiments

Figure 6 depicts final demonstration of our procedure on the data from electroporation experiments of attached cells. Electroporation efficiency is represented as a ratio between number of fluorescent cells and the total number of cells counted on the phase contrast images. We observe increase in the number of fluorescence cells with increasing field amplitude. If we compare manually determined electroporation efficiency with electroporation efficiency determined by our automated cell counting we observe excellent agreement of corresponding curves. This clearly demonstrates applicability of our automated counting procedure. The relative error of automated cell counting of those three experiments was, however, on average 8.53% for phase contrast images (what is in the range of interpersonal error 7.40%) and 7.64% for fluorescence images.

Discussion

In this paper, we present a technique for effective automated counting of attached and nonuniformly distributed cells in phase contrast images. This novel technique is robust enough against changes in cell shape and other optical characteristics and could thus be also used for live cell imaging and analysis of large number of images obtained by automatic image acquisition. We identified the ITCN

© 2010 The Authors

Table 5. Presentations of all results.

Average procedure error	Procedure's computer time	First inter-person error	Human effective counting time	Second inter-person error	Global minimum error	Computer time for global minimum error
$9.69 \pm 7.34\%$	<18 min	$6.55 \pm 3.67\%$	≈10 h	$10.57 \pm 3.25\%$	$7.99 \pm 6.37\%$	≈3 weeks

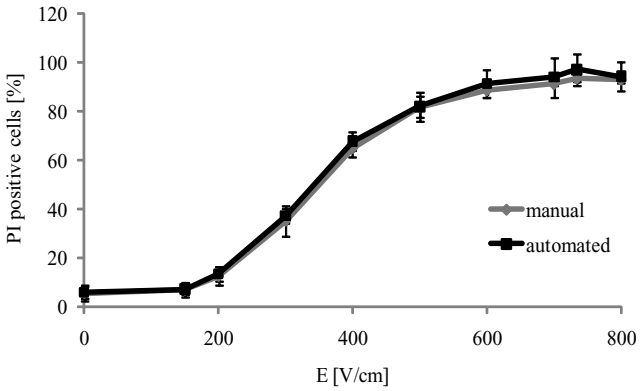

Fig. 6. Comparison of electroporation efficiency determined by manual cell counting to this determined by automated cell counting procedure. Data points represent mean and standard deviation of three independent experiments.

algorithm as appropriate cells detection tool. To effectively perform cell counting, the ITCN algorithm requires set up of the three parameters, which are obtained by ANN. We introduced a novel solution, where network input is fed by the normalized procedure error and the network outputs are the ITCN algorithm parameters. Furthermore, the automated procedure for counting of attached cells in phase contrast and also fluorescent images based on this smart optimization of ITCN algorithm's parameters was tested in evaluation of electroporation experiments.

ITCN algorithm used for counting cells (Byun *et al.*, 2006) is a promising tool for automated determination of electroporation efficiency of attached cells. The main part of the procedure is parameter optimization based on random selection of the training set (less than 2% of images), which makes the procedure robust to variations in images quality and/or object characteristics without the need for new programming and/or modification of source code. This is an advantage to many other solutions, which often fail if new image types are analysed. The training set approach has also been used in another study (Hawkins *et al.*, 2006), where optimal model for counting of spots in ELISpot assay was developed. If we perform optimization without ANN, that is exhaustive approach with all 2541 parameter sets included seeking for optimal parameter set on the same 10 training sets, the error we get is on average larger ($11.20 \pm 8.01\%$). However the reduction in computing time is even more pronounced: the exhaustive approach takes at least 8–9 h because all (2541) parameters sets have to be processed (Usaj *et al.*, 2007) while proposed approach takes significantly lower computer time (less than 18 min). With smart optimization approach. we overcome difficulties of manual setting optimal values for estimation of cell diameter and minimum cell distance of attached cells.

Another advantage of our counting procedure is its simple initialization. There are commercial software products (MetaMorph, Bioquant, Image-Pro) as well freeware [CellC (Tampere University of Technolog, Tampere, Finland), ImageJ] that provide object-counting and feature detection. We compared three tools (MetaMorph, Image-Pro, CellC) for cell counting using our image database containing 158 images. The results obtained with these tools yielded 16–65% absolute relative error whereas the absolute relative error of our counting procedure was below 9%.

What is perhaps even more important, these tools require intensive user interaction to obtain initialization or parameter settings for accurate results (Byun *et al.*, 2006). By contrast, initialization of our procedure is simple to perform. We only have to select parameter boundaries and count cells on (three) randomly selected training images. Moreover, because algorithm's parameters can be modified for each task and because they are directly related to object characteristics, the proposed procedure can be used in a variety of sample preparations or imaging methods, indicating its widespread applicability. This is demonstrated also in our study with successful evaluation of electroporation experiments that also includes counting of cells in fluorescence images.

The proposed procedure is very useful and could be effective in all areas where object counting is an everyday routine. However, there are some disadvantages at current development stage, which have to be mentioned.

Namely, when optimal parameter set is obtained it is used for all image data not taking into account variability between images. From Fig. 5, we can see that optimal parameters obtained in such a way are actually optimal for images with maximum cell density 150 cells per image while images with more cells need slightly different optimal parameters set. Higher cell density results in change of parameter minimal cell distance due to closer packing of the cells in the more confluent cell culture.

Another drawback of described procedure lies in template-matching approach with one template for all objects in images. Parameter 'cell size' here is the critical one. In our case, the problems are in one hand fused cells, which means that several

© 2010 The Authors

individual cells have fused into one giant cell (because of this reason extremely large, i.e. giant cells have been already excluded from test images). These giant cells are in principle over-counted. By contrast, there was also an undercounting problems found in confluent cell culture, due to high density of cells in images. It need to be stressed, however, that in confluent cell culture it is difficult to obtain exact number of cells even by manual counting performed by experienced user. In confluent cell culture, cells have consecutively the smallest size/area. Fused cells and confluent cell culture are found in images with high number of cells, therefore the counting error increases with number of cells, as we can observe in Fig. 5.

Our goal is to further improved method that will not only distinguish between images with small and high number of cells, but each image will be processed with its own optimal parameter set and template that will take care of both problems mentioned earlier. We are planning to engage more sophisticated heuristic optimization approach, such as genetic algorithm and ant-colony optimization to ignore local optimum trap, but consequently they will take more computer time. The challenge lies, however, also in the increasing processing speed towards the real-time.

When we want to asses and justify the accuracy of our automated procedure, we have to stress that there is no standard method of cell counting in phase contrast images to which automated methods could be compared. In the absence of such a standard evaluation, an expert opinion (with all of its associated subjectivity) represents the standard to which automated methods are evaluated (Hawkins *et al.*, 2006). The accuracy of automated counting method refers to how faithfully the method replicates the count from the expert. Image processing techniques usually have large amount of parameters, which have to be precisely tuned to get reliable results. Therefore direct comparison of global image analysis software is difficult because results from image analysis can be heavily skewed by how software is tuned. Besides, commercial software package are numerous and expensive. The algorithms in commercial software are also proprietary and protected so we cannot know how actually they work. For that reason they cannot be directly compared apart from the entire software package. The best evaluation of any new algorithm is, therefore, comparison with so-called gold standard such as manual counting, visual inspection and Coulter particle counters (Carpenter *et al.*, 2006).

We thus created our own image database with defined inter-person error and global minimum error to objectively assess our counting procedure. The average relative error between average cell numbers of three manual counting and our procedure (9.69%) is comparable to variation of manual counting as inter-person error is up to 10%. The advantage of automatic counting is the fact that it substantially reduces human counting time. Experimentally, we estimated average time for manual counting to be four minutes per image which gives approximately 10 h for 158 images. With the described method, manual counting time is reduced to 12 min. The error of automated counting can be significantly decreased (to 4%) if one training set per each experiment is chosen and if the illumination, the focus, the cell density (not too dense) and cell morphology (not too large) are taking care of during acquisition of images. In addition, taking into account global optimum error (7.99%) and procedure's systematic error (9.69%) and time needed to achieve global optimum (3 weeks), the performances of our optimization approach as well of described counting procedure are acceptable. Finally, we should mention that the procedure was quickly initialized and successfully used also for fluorescence image counting. This makes possible automated determination of electroporation efficiency as can be seen in Fig. 6, where good agreement with manual counting was obtained. Our image database is available as a supplemental material that other researchers in this field could compare their counting tools with.

Conclusions

Automated measurement from microscopy images is an important tool in biotechnology and biomedicine. The procedure we describe here for automated cell counting in phase contrast images is especially useful on large numbers of images. The presented procedure at its current development produces reasonably good and acceptable results. Average procedure's systematic error is 9.69%, which is comparable to manual counting inter-person error. With our smart parameter optimization approach, the need of human intervention (counting time and ITCN algorithm initialization) is reduced considerably nevertheless comparable results are achieved. The procedure can be successfully used also for fluorescence image counting and thus for automated determination of electroporation efficiency.

Acknowledgements

This research was supported by the Slovenian Research Agency (ARRS). Authors thank to Jiyun Byun, Center for BioImage Informatics, University of California, for providing us with MATLAB source code and her help in tuning algorithm's parameters. The authors also thank students and employees in Laboratory of Biocybernetics for manual counting of cells and especially to Alenka Macek-Lebar, Ph.D., for helpful and fruitful discussions during the preparation of this work. The authors also thank Prof. Bostjan Likar, Ph.D., for helpful discussion and providing an application for retrospective shading correction.

References

Ambriz-Colin, F., Torres-Cisneros, M., Avina-Cervantes, J.G., Saavedra-Martinez, J.E., Debeir, O. & Sanchez-Mondragon, J.J. (2006) Detection

© 2010 The Authors

of biological cells in phase-contrast microscopy images. In: *Proceedings of the IEEE MICAI*. IEEE Computer Society, Washington.

Andre, F. & Mir, L.M. (2004) DNA electrotransfer: its principles and an updated review of its therapeutic applications. *Gene Ther.* **11**, S33–S42.

Byun, J.Y., Verardo, M.R., Sumengen, B., Lewis, G.P., Manjunath, B.S. & Fisher, S.K. (2006) Automated tool for the detection of cell nuclei in digital microscopic images: application to retinal images. *Mol. Vis.* **12**, 949–960.

Canatella, P.J., Karr, J.F., Petros, J.A. & Prausnitz, M.R. (2001) Quantitative study of electroporation-mediated molecular uptake and cell viability. *Biophys. J.* **80**, 755–764.

Carpenter, A., Jones, T., Lamprecht, M., *et al.* (2006) CellProfiler: image analysis software for identifying and quantifying cell phenotypes. *Genome Biol.* **7**, R100–R100.10.

Chen, X.W., Zhou, X.B. & Wong, S.T.C. (2006) Automated segmentation, classification, and tracking of cancer cell nuclei in time-lapse microscopy. *IEEE Trans. Biomed. Eng.* **53**, 762–766.

Debeir, O., Van Ham, P., Kiss, R. & Decaestecker, C. (2005) Tracking of migrating cells under phase-contrast video microscopy with combined mean-shift processes. *IEEE Trans. Med. Image.* **24**, 697–711.

Embleton, K.V., Gibson, C.E. & Heaney, S.I. (2003) Automated counting of phytoplankton by pattern recognition: a comparison with a manual counting method. *J. Plankton Res.* **25**, 669–681.

Gabrijel, M., Bergant, M., Kreft, M., Jeras, M. & Zorec, R. (2009) Fused late endocytic compartments and immunostimulatory capacity of dendritic—tumor cell hybridomas. *J. Membr. Biol.* **229**, 11–18.

Gehl, J. & Geertsen, P.F. (2006) Palliation of haemorrhaging and ulcerated cutaneous tumours using electrochemotherapy. *Eur. J. Cancer. Suppl.* **4**, 35–37.

Golzio, M., Rols, M.P., Gabriel, B. & Teissie, J. (2004) Optical imaging of in vivo gene expression: a critical assessment of the methodology and associated technologies. *Gene Ther.* **11**, S85–S91.

Haralick, R.M. & Shapiro, L.G. (1985) Image segmentation techniques. *Comput. Vis. Graph Image Process.* **29**, 100–132.

Hawkins, N., Self, S. & Wakefield, J. (2006) The automated counting of spots for the ELISpot assay. *J. Immunol. Methods* **316**, 52–58.

Hayashi, T., Tanaka, H., Tanaka, J., Wang, R., Averbook, B.J., Cohen, P.A. & Shu, S. (2002) Immunogenicity and therapeutic efficacy of dendritic-tumor hybrid cells generated by electrofusion. *Clin. Immunol.* **104**, 14–20.

Jacobs, J.J.L., Lehe, C., Cammans, K.D.A., Yoneda, K., Das, P.K. & Elliott, G.R. (2001) An automated method for the quantification of immunostained human Langerhans cells. *J. Immunol. Methods* **247**, 73–82.

Kandušer, M. & Miklavčič, D. (2008) Electroporation in biological cell and tissue: an overview. *Electrotechnologies for Extraction from Food Plants and Biomaterials* (ed. by E. Vorobiev & N. Lebovka). Springer Science, New York.

Li, K., Miller, E.D., Weiss, L.E., Campbell, P.G. & Kanade, T. (2006) Online tracking of migrating and proliferating cells imaged with phase-contrast microscopy. In *Proceedings of the IEEE Conference Computer Vision and Pattern Recognition Workshop*. IEEE Computer Society Press, Los Alamitos.

Likar, B., Maintz, J.B.A., Viergever, M.A. & Pernus, F. (2000) Retrospective shading correction based on entropy minimization. *J. Microsc.* **197**, 285–295.

Macek-Lebar, A. & Miklavcic, D. (2001) Cell electropermeabilization to small molecules in vitro: control by pulse parameters. *Radiol. Oncol.* **35**, 193–202.

Marty, M., Sersa, G., Garbay, J.R., *et al.* (2006) Electrochemotherapy – an easy, highly effective and safe treatment of cutaneous and subcutaneous metastases: results of ESOPE (European Standard Operating Procedures of Electrochemotherapy) study. *Eur. J. Cancer Suppl.* **4**, 3–13.

Masters, T. (1995) *Advanced Algorithms for Neural Networks: A C++ Sourcebook*. John Wiley & Sons Inc., New York.

Mir, L.M., Gehl, J., Sersa, G., *et al.* (2006) Standard operating procedures of the electrochemotherapy: instructions for the use of bleomycin or cisplatin administered either systemically or locally and electric pulses delivered by the Cliniporator (TM) by means of invasive or non-invasive electrodes. *Eur. J. Cancer Suppl.* **4**, 14–25.

Neumann, E., Kakorin, S. & Toensing, K. (1999) Fundamentals of electroporative delivery of drugs and genes. *Bioelectrochem. Bioenerg.* **48**, 3–16.

Neumann, E., Sowers, A.E. & Jordan, C.A. (1989) *Electroporation and Electrofusion in Cell Biology*. Springer-Verlag, New York.

Pavselj, N. & Preat, V. (2005) DNA electrotransfer into the skin using a combination of one high- and one low-voltage pulse. *J. Control. Release* **106**, 407–415.

Pucihar, G., Mir, L.M. & Miklavcic, D. (2002) The effect of pulse repetition frequency on the uptake into electropermeabilized cells in vitro with possible applications in electrochemotherapy. *Bioelectrochemistry* **57**, 167–172.

Rols, M.P. (2006) Electropermeabilization, a physical method for the delivery of therapeutic molecules into cells. *Biochim. Biophys. Acta Biomembr.* **1758**, 423–428.

Rols, M.P. & Teissie, J. (1992) Experimental-evidence for the involvement of the cytoskeleton in mammalian-cell electropermeabilization. *Biochim. Biophys. Acta* **1111**, 45–50.

Rubinsky, B., Onik, G. & Mikus, P. (2007) Irreversible electroporation: a new ablation modality-clinical implications. *Technol. Cancer Res. Treat.* **6**, 37–48.

Rumelhart, D.E., Hinton, G.E. & Williams, R.J. (1986) Learning internal representations by error propagation. *Parallel Distributed Processing: Explorations in the Microstructure of Cognition*, vol. 1 (ed. by D.E. Rumelhart & J.L. McClelland). MIT Press, Cambridge, MA.

Russ, J.C. (1995) *The Image Processing Handbook*, 2nd edn. IEEE Press, Boca Raton, FL.

Sersa, G., Miklavcic, D., Cemazar, M., Rudolf, Z., Pucihar, G. & Snoj, M. (2008) Electrochemotherapy in treatment of tumours. *Eur. J. Surg. Oncol.* **34**, 232–240.

Steenstrup, T., Clase, K.L. & Hannon, K.M. (2000) Rapid quantification of cell numbers using computer images. *Biotechniques* **28**, 624–626.

Teissie, J. & Rols, M.P. (1993) An experimental evaluation of the critical potential difference inducing cell-membrane electropermeabilization. *Biophys. J.* **65**, 409–413.

Theera-Umpon, N. & Gader, P.D. (2002) System-level training of neural networks for counting white blood cells. *IEEE Trans. Syst., Man, Cybern. C, Appl. Rev.* **32**, 48–53.

Thimm, G., Moerland, P. & Fiesler, E. (1996) The interchangeability of learning rate and gain in backpropagation neural networks. *Neural Comput.* **8**, 451–460.

Tomazevic, D., Likar, B. & Pernus, F. (2002) Comparative evaluation of retrospective shading correction methods. *J. Microsc.* **208**, 212–223.

Trontelj, K., Rebersek, M., Kanduser, M., Serbec, V.C., Sprohar, M. & Miklavcic, D. (2008) Optimization of bulk cell electrofusion in vitro for production of human-mouse heterohybridoma cells. *Bioelectrochemistry*, **74**, 124–129.

© 2010 The Authors

Tsong, T.Y. (1991) Electroporation of cell-membranes. *Biophys. J.*, **60**, 297–306.

Usaj, M., Torkar, D. & Miklavcic, D. (2007) Automatic cell detection in phase-contrast images for evaluation of electroporation efficiency in vitro. *IFMBE Proceedings* (ed. by T. Jarm, P. Kramar & A. Zupanic). Springer, Berlin, Heidelberg.

Vovk, U., Pernus, F. & Likar, B. (2007) A review of methods for correction of intensity inhomogeneity in MRI. *IEEE Trans. Med. Imaging* **26**, 405–421.

Wang, S.T. & Min, W. (2006) A new detection algorithm (NDA) based on fuzzy cellular neural networks for white blood cell detection. *IEEE Trans. Inf. Technol. Biomed.* **10**, 5–10.

Weaver, J.C. & Chizmadzhev, Y.A. (1996) Theory of electroporation: a review. *Bioelectrochem. Bioenerg.* **41**, 135–160.

Wu, K.N., Gauthier, D. & Levine, M.D. (1995) Live cell image segmentation. *IEEE Trans. Biomed. Eng.* **42**, 1–12.

Yang, X.D., Li, H.Q. & Zhou, X.B. (2006) Nuclei segmentation using marker-controlled watershed, tracking using mean-shift, and Kalman filter in time-lapse microscopy. *IEEE Trans. Circuits Syst. Regul. Paper* **53**, 2405–2414.

Yongming, C., Biddell, K., Aiying, S., Relue, P.A. & Johnson, J.D. (1999) An automatic cell counting method for optical images. In *Proceedings of the IEEE of the First Joint BMES/EMBS Conference*, Atlanta, U.S.A.

Yu, X., McGraw, P.A., House, F.S. & Crowe, J.E., Jr. (2008) An optimized electrofusion-based protocol for generating virus-specific human monoclonal antibodies. *J. Immunol. Methods.* **336**, 142–151.

Zupanic, A. & Miklavcic, D. (2010) Optimization and numerical modeling in irreversible electroporation treatment planning. *Irreversible Electroporation* (ed. by B. Rubinsky). Springer-Verlag, Berlin, Heidelberg.

Appendix

Short ITCN protocol for microscope user:

1. From images acquired during each experiment select the training set (recommended at least three images); try to acquire as much quality images as possible, at least avoid poor focus, dirties, cell remainders and fused cells.
2. Perform manual cell counting on images in training set.
3. Set the minimum and maximum value of ITCN tools parameters (cell size, minimal cell distance, threshold).
4. Run optimization with appropriate input data (real cell numbers from training image set and parameters borders).
5. Perform automated cell counting of the rest of the images using ITCN tools with obtained optimal parameters.

© 2010 The Authors